PCCP

Accepted Manuscript

This is an *Accepted Manuscript*, which has been through the Royal Society of Chemistry peer review process and has been accepted for publication.

Accepted Manuscripts are published online shortly after acceptance, before technical editing, formatting and proof reading. Using this free service, authors can make their results available to the community, in citable form, before we publish the edited article. We will replace this *Accepted Manuscript* with the edited and formatted *Advance Article* as soon as it is available.

You can find more information about *Accepted Manuscripts* in the **Information for Authors**.

ROYAL SOCIETY OF CHEMISTRY

www.rsc.org/pccp

Layer-by-Layer fabrication of AgCl-PANI hybrid nanocomposite films for electronic tongues

Alexandra Manzoli,[1*] Flavio M. Shimizu,[1,2] Luiza A. Mercante,[1] Elaine C. Paris,[1]
Osvaldo N. Oliveira Jr.,[2] Daniel S. Correa,[1*] Luiz H. C. Mattoso[1]

[1]*National Laboratory for Nanotechnology in Agribusiness (LNNA), Embrapa
Instrumentação, 13560-970, São Carlos, SP, Brazil*
[2]*São Carlos Institute of Physics, University of São Paulo (USP), PO Box 369, 13566-
590, São Carlos, SP, Brazil*

* Corresponding authors: e-mail: daniel.correa@embrapa.br (D.S. Correa) and
alexxiamanzoli@gmail.com (A. Manzoli)

Abstract

The fabrication of nanostructured films with tailored properties is essential for many applications, particularly with materials such as polyanilines (PANI) whose electrical characteristics may be easily tuned. In this study we report the one-step synthesis of AgCl-PANI nanocomposites that could form layer-by-layer (LbL) films with poly(sodium 4-styrenesulfonate) (PSS) and be used for electronic tongues (e-tongues). The first AgCl-PANI layer was adsorbed on a quartz substrate according to a nucleation-and-growth mechanism explained with the Johnson–Mehl–Avrami (JMA) model, revealing a 3D film growth confirmed with atomic force microscopy (AFM) measurements for the AgCl-PANI/PSS LbL films. In contrast to conventional PANI-containing films, the AgCl-PANI/PSS LbL films deposited on interdigitated electrodes exhibited electrical resistance that was practically unaffected by changes in pH from 4 to 9, and therefore these films can be used in e-tongues for both acidic and basic media. With a sensor array made of AgCl-PANI/PSS LbL films with different numbers of bilayers, we demonstrated the suitability of the AgCl-PANI nanocomposite for an e-tongue capable of clearly discriminating the basic tastes from salt, acid and umami solutions. Significantly, the hybrid AgCl-PANI nanocomposite is promising for any application in which PANI de-doping at high pH is to be avoided.

Introduction

A judicious choice of sensing materials and film architectures is essential for reaching high performance in chemical sensor arrays such as those employed in electronic tongues (e-tongues). Such approach allows one to explore the cross-sensitivity afforded by nanostructured films with distinct electrical characteristics.[1] Among the many candidate materials for such tasks are the semiconducting polymers that may be useful in various other applications where corrosion inhibition or antistatic properties are required. They may also be useful in light-emitting diodes, solar cells and smart sensors.[2] Of particular relevance is the polyaniline (PANI) family, whose electrical properties can be tuned by controlling their doping level through simple non-redox acid doping and base de-doping process. Indeed, the emeraldine oxidation form is reversibly switched between electrically insulating emeraldine base and conducting emeraldine salt forms.[3] The PANI conductivity can therefore be altered rather easily for tailored applications. PANI is particularly suitable for distinguish flavors with small changes in acidity. However, this pH dependence may be a problem for using PANI as active layer in chemical sensors since de-doping at high pH may compromise the reusability of the sensing unit.[4]

The main challenge in taking full advantage of PANI properties for e-tongues is to find ways to reduce the pH dependence while keeping a high sensitivity to changes in the electric properties of liquid samples. A possibility that emerged is the fabrication of hybrid organic-inorganic nanocomposites, which avoids doping/de-doping of PANI with respect to pH making them useful for neutral or even basic analytes.[5] With such flexibility in properties, hybrid PANI nanocomposites have indeed been used in electronic applications, including as active layer for chemical sensors.[6] The sensing units in e-tongues are generally obtained by deposition of a thin active layer onto an electrode to interact with the analyte. Several film fabrication methods have been proposed for this purpose,[7] and perhaps the most commonly used now is the Layer-by-Layer (LbL) technique owing to its experimental simplicity and low cost.[8]

Here we report a chemical sensor array with reduced pH dependence that can be successfully fabricated with LbL films made from AgCl-PANI hybrid nanocomposites synthesized by a one-step route. This sensor array comprised AgCl-PANI/PSS LbL films with 3, 5 and 7 bilayers and a bare electrode that operated on the principle of impedance spectroscopy. The new e-tongue utilized Principal Component Analysis and

was capable of discriminating flavors in solutions with a broad pH range with good performance.

Experimental

Synthesis of AgCl-PANI nanocomposites

AgCl-PANI nanocomposites were synthesized by a one-step process[9] in the presence and absence of the shape control agent poly(vinylpyrrolidone) (PVP), and using two precursors: silver nitrate ($AgNO_3$) and silver sulfate ($AgSO_4$). A solution of 0.012 mol L^{-1} precursor and 0.012 mol L^{-1} aniline monomer, which had been distilled under reduced pressure and stored at low temperature, were added in a 4% PVP aqueous solution under stirring. A HCl aqueous solution at 1 mol L^{-1} of ammonium persulfate (APS) as oxidant was dropped into the resultant mixture using a 1:1 molar ratio (aniline:APS). These reacting substances were left under stirring for 24 h at room temperature and then the precipitate was centrifuged and washed several times with distilled water and ethanol. The final product was lyophilized for 2 h and stored in a desiccator.

Preparation of AgCl-PANI/PSS LbL films

A solution of 1 mg mL^{-1} AgCl-PANI was prepared by dispersing the nanocomposites in 1 mL dimethylacetamide (DMAc) under stirring for 10 min, and then 9 mL of HCl aqueous solution (pH 3) were added. Poly(sodium 4-styrenesulfonate) (PSS) solution was dissolved in HCl (pH 3). AgCl-PANI/PSS LbL films were deposited on quartz, silicon wafers and platinum interdigitated electrodes by alternating immersion into cationic AgCl-PANI and PSS anionic solutions.

Nanocomposite and film characterization

AgCl-PANI nanocomposites were characterized by X-ray diffraction (XRD) using a Shimadzu XRD 6000 diffractometer with CuKα radiation from 10° to 80° (2θ) at 2° min^{-1}. The morphology of as-prepared samples was observed using a field-emission gun scanning electron microscopy FEG-SEM (JEOL-JSM 6701F). The morphology and thickness of LbL films adsorbed on a glass substrate were assessed by AFM using a Dimension V (Veeco) microscope. All images were obtained in the Tapping[TM] mode with scan rate of 0.6 Hz, using silicon nitride tips attached to a cantilever of spring constant of 2.5 N m^{-1}. The film thickness was determined using a

scalpel to scratch and peel out a small spot of the film deposited onto a glass substrate. The root-mean-square roughness (R_{rms}) was calculated using Gwydion$^{©}$ 2.1 data analysis software. UV–Vis absorption spectra were recorded with a Perkin-Elmer Lambda 25 on quartz slides. FTIR spectroscopy was performed on a Perkin-Elmer 1000 using silicon wafers as substrates for the films. A total of 64 scans were collected with a resolution of 4 cm^{-1}. Electrical characterization of sensing units was performed using an impedance gain phase analyzer (Solartron, model 1260). Data were collected in the range from 1 Hz up to 1 MHz, with an ac applied signal of 50 mV amplitude.

Results and Discussion

The synthesis of hybrid nanocomposites employed $AgNO_3$ and Ag_2SO_4 as precursors, in the presence and absence of the shape control agent (PVP). The XRD patterns in Figure 1 correspond to the crystal planes of inorganic, face-centered cubic (FCC) crystals of AgCl nanoparticles, in good agreement with the data in JCPDS File No. 06-0480. For the synthesis in the presence of PVP, the baseline changed in the region from 10° to 35° assigned to amorphous PANI, thus suggesting the formation of AgCl-PANI nanocomposites. This is consistent with Feng et al.[9] who showed that AgCl-PANI nanocomposites could not be formed without PVP because interaction between inorganic AgCl nanoparticles and the aniline monomer was promoted by the amphiphilic PVP. The mechanism in the interaction, according to Hao et al.,[10] consists in PVP being firstly attached onto the surface of the nanoparticles, then providing active sites to induce PANI growth. This type of interaction prevents PANI aggregation and limits nanoparticle growth, since the preferential alignment of monomer onto PVP leads to a larger number of hydrogen bonds between PANI-PVP than PANI-PANI.[11]
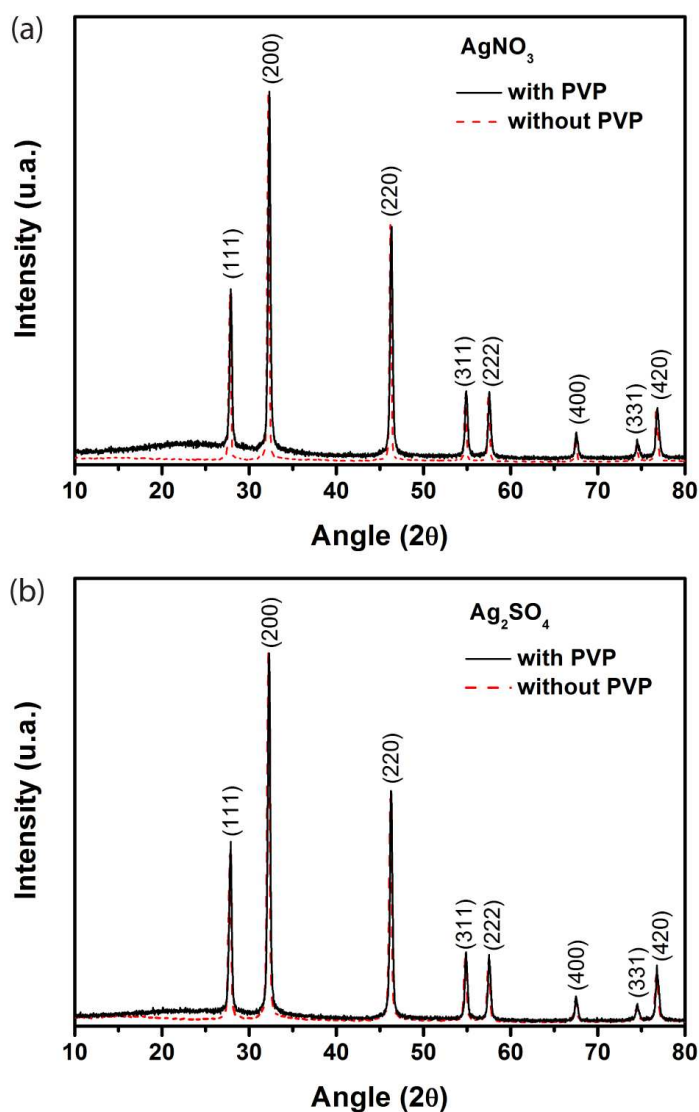
FIGURE 1. X-ray Powder diffraction (XRD) patterns for AgCl-PANI nanocomposites obtained by one-step process in the presence and absence of PVP with (a) AgNO$_3$ and (b) Ag$_2$SO$_4$ precursors.

The average size of the AgCl nanoparticles was calculated using Scherrer's equation for the most intense diffraction peak (200), and confirmed the influence from PVP, which induced smaller crystallites when AgNO$_3$ was used as precursor. The average size D, in nm, was: $D_{AgNO3} = 48$, $D_{AgNO3/PVP} = 30$, $D_{Ag2SO4} = 32$ and $D_{Ag2SO4/PVP} = 32$. Similar effects were reported by Soltani *et al.*[12] with the size of zinc sulfide nanoparticles being limited by increasing concentrations of PVP. According to the authors, the coordination of PVP through its nitrogen atom can provide the capping effect to limit nanoparticle growth.

6

The effect from PVP on the morphology of nanocomposites was confirmed in the FEG-SEM images of Figure 2, where reduced size AgCl-PANI nanocomposites are shown for the PVP-containing synthesis, consistent with the XRD results. The decrease in particle size is an interesting feature for the nanocomposites to be exploited in sensing units, for a larger area/volume ratio usually favors sensitivity. Therefore, for the sensing applications we employed the LbL films containing AgCl-PANI nanocomposites prepared with $AgNO_3$ in the presence of PVP.
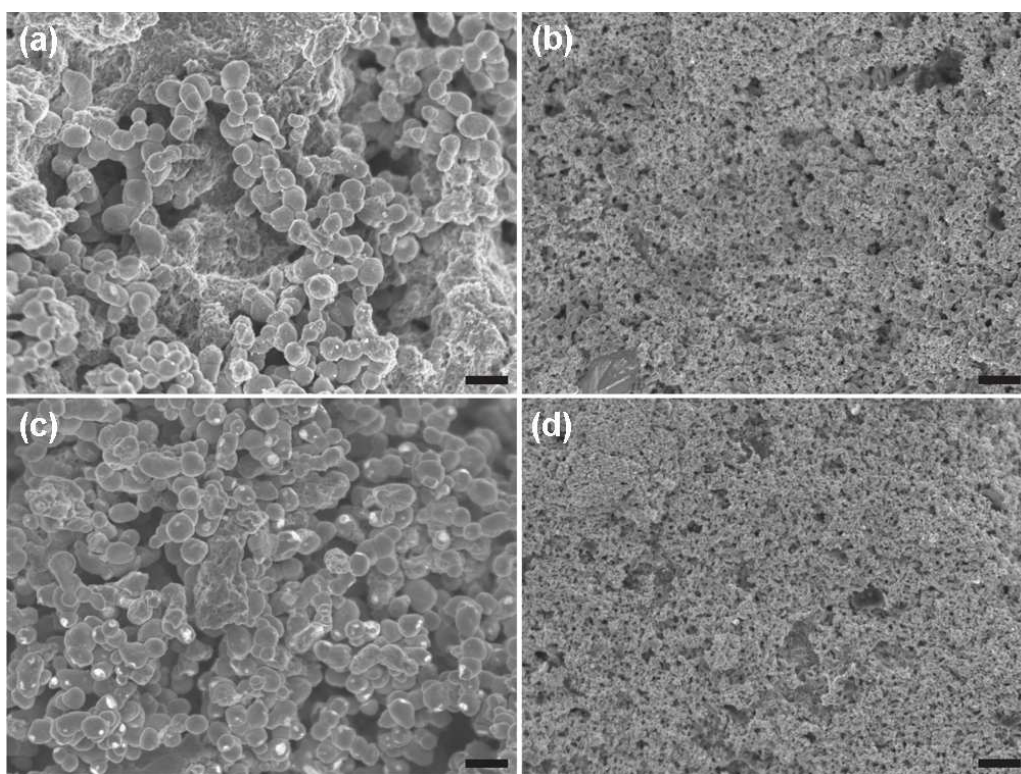
FIGURE 2. FEG-SEM images of the AgCl-PANI nanocomposites. Conditions: (a) $Ag_2(SO_4)$, (b) $Ag_2(SO_4)$ with PVP, (c) $AgNO_3$ and (d) $AgNO_3$ with PVP (scale bar = 1 μm).

The adsorption mechanism of the first layer of AgCl-PANI onto the quartz substrate to form the LbL film was interpreted using a model based on the Johnson–Mehl–Avrami (JMA) equation,[13] which gives a phenomenological description of adsorption kinetics and has been successfully applied to polymer film growth.[14] The adsorbed mass is assumed to be proportional to the optical absorbance, defined in the JMA equation by

$$A = k_1 \left(1 - \exp\left(\frac{-t}{\tau_1}\right) \right) + k_2 \left(1 - \exp\left(-\left(\frac{t}{\tau_2}\right)^n \right) \right) \quad (1)$$

where A is the absorbance at a selected wavelength, k and n are constants, τ_1 and τ_2 are the characteristic times. The first exponential corresponds to a first-order kinetics with τ_1 being associated with nucleation of polymer domains, while τ_2 is related to growth of already-formed nuclei. The second exponential cannot be of first-order because the increase in absorbance after the plateau has an upward inflexion. The adsorption kinetics curve for the AgCl-PANI layer in Figure 3 reveals saturation of polymer adsorption after 300 s, consistent with $\tau_2 = 345$ s. The value n = 3 corresponds to a 3D growth of spheroids.[15]
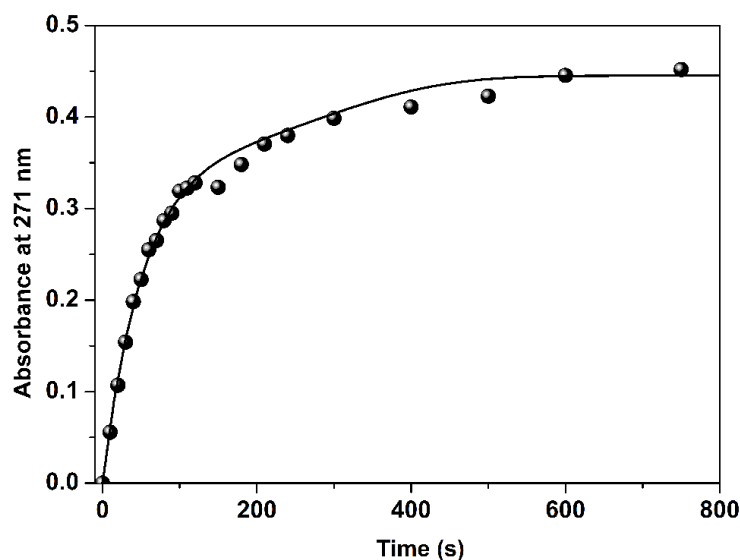
FIGURE 3. Adsorption kinetics curve for the first AgCl-PANI layer deposited onto a quartz substrate. The solid lines represent the fit using the JMA model.

The sequential growth of AgCl-PANI/PSS LbL films prepared with an immersion time of 345 s was monitored by UV-Vis spectroscopy. The two peaks in the spectra at 271 and 840 nm in Figure 4(a) are assigned to the π-π* transition of the benzenoid and quinoid rings on the PANI chain.[16] The absorbance increased linearly with the number of bilayers, as indicated in Figure 4(b), and therefore the same amount of material was adsorbed in each bilayer.
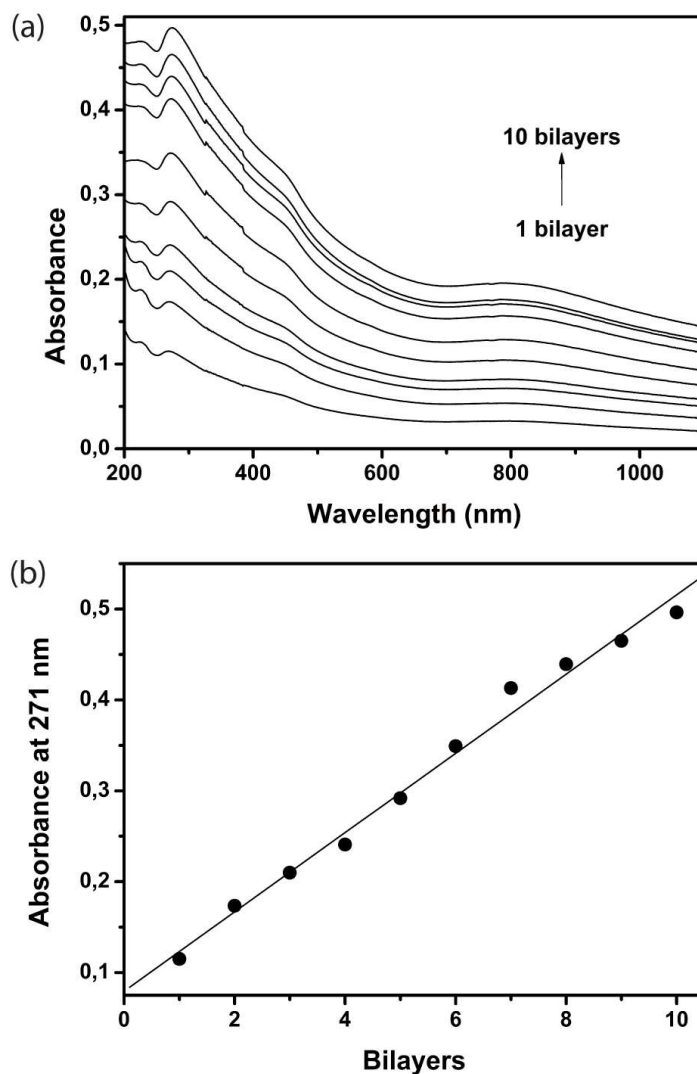
FIGURE 4. (a) UV-Vis absorption spectra for the layer-by-layer films of AgCl-PANI/PSS, ranging from 1 up to 10 bilayers and (b) Absorption at 271 nm as a function of the number of deposited bilayers, displaying the linear dependence.

The AFM images in Figure 5 show a globular morphology typical of polyanilines,[17] also featuring nuclei growth as the number of AgCl-PANI/PSS bilayers increased from 3 to 7. Such growth is accompanied by an increased roughness (R_{rms}), with R_{rms} = 38 nm, 42 nm and 52 nm for 3, 5 and 7 bilayers, respectively. The increased globule size and roughness are consistent with the 3D growth in film deposition as determined with the JMA model. The AFM was also used to measure the film thickness and the obtained values were: 66, 119 and 259 nm for 3, 5 and 7 bilayers, respectively.
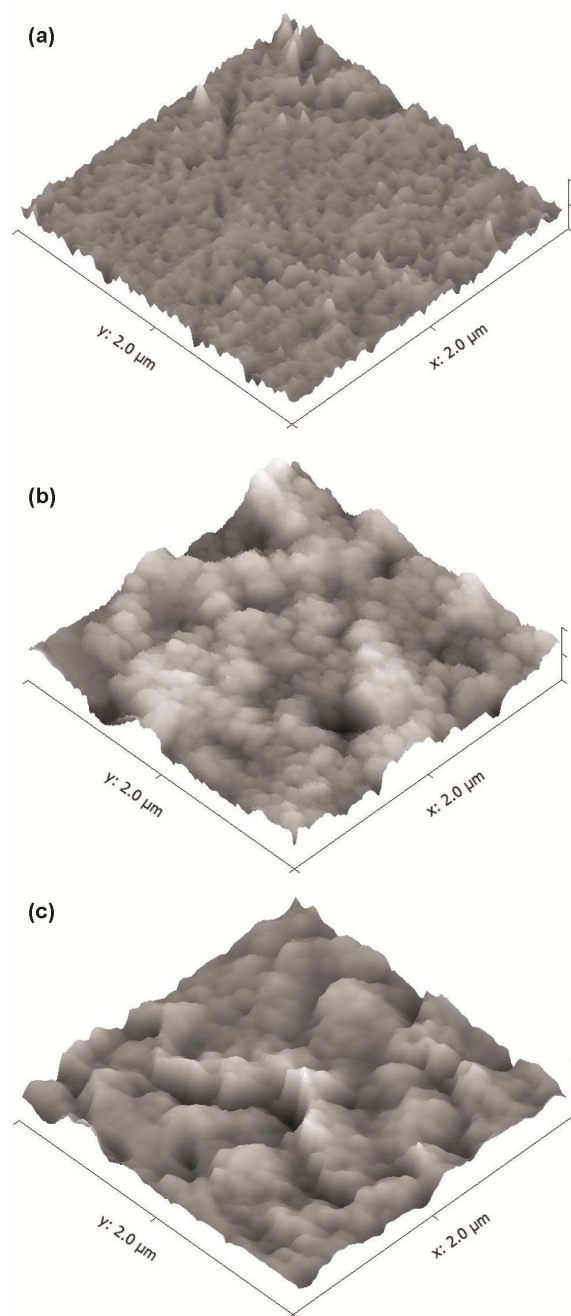
FIGURE 5. AFM 3D images of (a) 3, (b) 5, and (c) 7-bilayer AgCl-PANI/PSS LbL films. LbL films with these three thicknesses were studied because these were the numbers of bilayers used in the sensor array for an e-tongue discussed later on.

The successful adsorption of both components on the LbL film was confirmed by comparing the FTIR spectrum for a 5-bilayer AgCl-PANI/PSS LbL film with spectra taken for PSS and AgCl-PANI cast films. Figure 6 displays the main vibrational bands of AgCl-PANI assigned as follows. 1588-1570 cm^{-1} (C=C stretching of quinoid rings),

1490-1508 cm^{-1} (C=C stretching of benzenoid rings), 1308 cm^{-1} (stretching vibration of the secondary amine C–N group), 1150 cm^{-1} (ring amine bending vibrations modes) and 832 cm^{-1} (C–H out-of-plane deformation vibration of the benzenoid groups).[15,18] The sulfonic group vibration bands at 1010 and 1038 cm^{-1} in the AgCl-PANI/PSS LbL film spectrum confirms the presence of PSS in the LbL film. The bands at 1588 cm^{-1} and at 1490 cm^{-1} in the AgCl-PANI cast film spectrum are shifted by 18 cm^{-1} to lower and higher wavenumbers, respectively, in the AgCl-PANI/PSS LbL films. These changes in the LbL film result from electrostatic interactions between AgCl-PANI and PSS, probably involving the quinoid groups of PANI.[19]
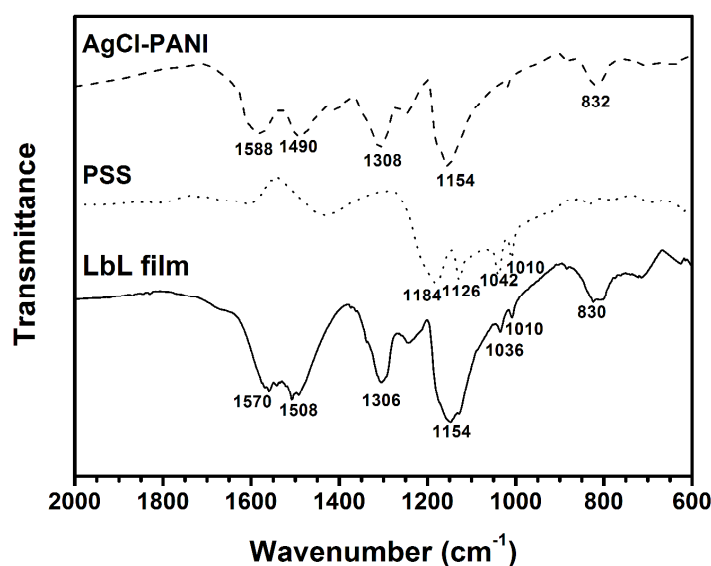
FIGURE 6. FTIR spectra of AgCl-PANI/PSS LbL film, PSS and AgCl-PANI cast films.

Electrical characterization

The main motivation in this study was to obtain a polyaniline-based sensing unit that would keep the sensing ability for a chemical sensor, without being affected by drastic changes in pH in order to increase reusability. To demonstrate that this aim was fulfilled we used as a model two types of nanostructured films then measured and compared their electrical impedance: (i) 5-bilayer AgCl-PANI/PSS LbL film and (ii) 5-bilayer commercial PANI/PSS LbL film. The measurements were taken from 1 Hz to 1 MHz with the sensing units immersed into solutions with pH varying from 2 to 9. Figure 7 shows the electrical resistance (a) and capacitance (b) at 1 kHz, where the

capacitance was essentially unaltered between pH 4 and 9 for the nanocomposite film, whereas it varied up to 67% in the same pH range for the film containing commercial PANI. Most importantly, Figure 7(b) shows an abrupt change in resistance for commercial PANI, which as expected was rather low (0.5 to 4 kΩ) for acid media but then increased considerably in basic media, reaching hundreds of kΩ. This expected increase in resistivity arises from de-doping of PANI in basic media, and may have deleterious effects in sensing.[20] On the other hand, the sensing unit made with AgCl-PANI/PSS had a small change in resistance, which can be ascribed to addition of inorganic nanoparticles into the polymer. Although the mechanism that maintains AgCl-PANI nanocomposite stable in neutral media has not been fully elucidated, it is believed to be a consequence of the large amount of negative charged chloride ions. Such ions provide the anionic doping that yields a redox-active nanocomposite at neutral and even basic aqueous solution.[21]
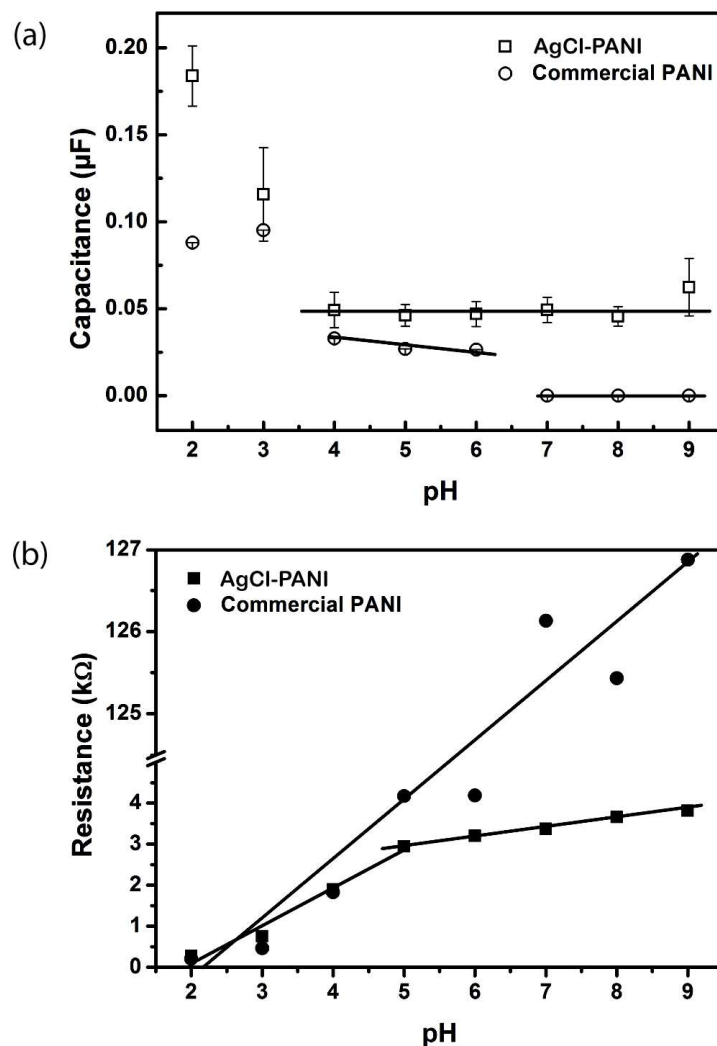
FIGURE 7. (a) Capacitance and (b) electrical resistance values measured at 1 kHz varying the solution pH from 2 to 9 for commercial PANI and AgCl-PANI nanocomposite film with 5 bilayers.

To demonstrate the suitability of the nanocomposite films for applications in chemical sensors, we tested them in an e-tongue array, whose units contained AgCl-PANI/PSS LbL films with 3, 5 and 7 bilayers and a bare electrode. Such approach provides a change in film thickness, which alters the electrical response for each sensing unit. This methodology can provide variability to establish a finger-printing pattern for a given liquid within the global selectivity concept.[22]

The electrical resistance for the sensing units immersed in solutions with concentrations 10^{-3}, 10^{-4} and 10^{-5} mol L^{-1} representing the basic tastes acid (HCl), salt (NaCl) and umami (glutamate) were treated with the statistical method Principal

Component Analysis (PCA). This method is a mathematical procedure that employs orthogonal transformations to convert a set of multivariate data into a set of values of uncorrelated variables called principal components.[23] The PCA plot in Figure 8 indicates full discrimination of all samples in distinct groups, including distilled water as a reference. For instance, we note that distilled water is located on the positive side of PC1 and negative side of PC2. Salty solutions (NaCl) are grouped in the same region as distilled water, however they are located in a well-separated cluster, which indicate a good discrimination. Acidic solutions (HCl) can be seen in a well-separated cluster located on the positive sides of PC1 and PC2, while glutamate solutions are grouped on the opposed region (negative sides of PC1 and PC2). Moreover, the data variance was mainly accounted using two first principal components, yielding 96 % (PC1 + PC2) of the total information collected by the array. Therefore, in addition to being unaffected to large changes in pH, the AgCl-PANI/PSS LbL films can clearly distinguish different basic flavors and be successfully employed in an e-tongue.
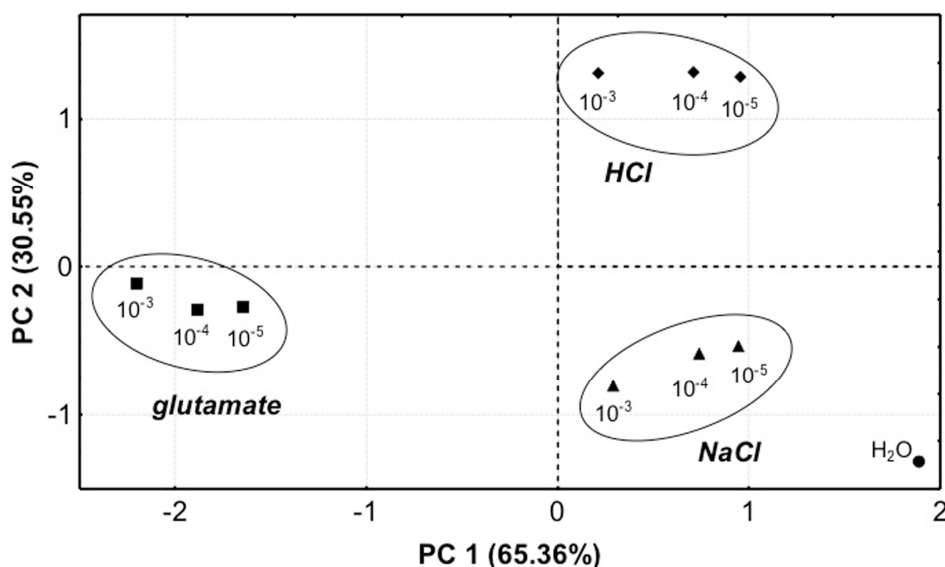
FIGURE 8. PCA plots for distilled water and the three flavors: acid (HCl), salty (NaCl) and umami (glutamate). The electrical resistance values were recorded at 1 kHz and 50 mV, using an e- tongue with four sensing units (bare electrode and electrodes with 3, 5 and 7 bilayers of AgCl-PANI/PSS LbL films). The data variance for PC1 and PC2 is included in parentheses. The frequency 1 kHz was chosen to analyze the data because normally higher sensitivity is achieved at lower frequencies owing to the importance of the electrical double-layer in the electrical response.[24]

In subsidiary experiments, we used a similar sensor array made with commercial PANI/PSS LbL films, also with 3, 5 and 7 bilayers, but discrimination of the basic tastes in the PCA plot was not adequate. This is further confirmation of the suitability of the AgCl-PANI nanocomposite LbL films for chemical sensor, whose performance was superior to that observed for commercial PANI. It should also be remarked that the sensivity reached here with the basic taste solutions down to 10^{-5} mol L^{-1} is not as high as in other studies (see for instance ref. 25), for we made no attempt to optimize the performance. Our focus was in demonstrating the suitability of AgCl-PANI nanocomposites for e-tongues, which can be applied to both acidic and basic media.

Conclusion

AgCl-PANI hybrid nanocomposites were obtained using $AgNO_3$ precursor in the presence of 4% PVP by one-step synthesis, which was confirmed by XRD and FEG-SEM measurements. Growth of the first AgCl-PANI layer on a quartz substrate could be explained using the JMA model, typical of nucleation and growth processes, consistent with film morphology of AgCl-PANI/PSS LbL films studied with AFM. The electrical properties of AgCl-PANI/PSS LbL films adsorbed on platinum interdigitated electrodes were almost unaffected by changes in pH from 4 to 9. In contrast, PANI/PSS films obtained with commercial PANI presented a drastic decrease in conductivity with pH, as a consequence of its de-doping process. Therefore, the AgCl-PANI nanocomposite was further employed in an e-tongue based on a sensor array comprising a bare electrode and electrodes coated with different numbers of AgCl-PANI/PSS LbL films. Using PCA to analyze the electrical resistance of the sensing units immersed in liquid solutions representing basic tastes, we show that the e-tongue was capable of discriminating salt, acid and umami solutions at a concentration of 10^{-5} mol L^{-1}. Taken together, these results indicate that the electrical properties of AgCl-PANI nanocomposite can be tailored for specific applications, as demonstrated here for an e-tongue that may be used in acidic as well as in basic media.

Acknowledgements

References

1 (a) M. Śliwińska, P. Wiśniewska, T. Dymerski, J. Namieśnik and W. Wardencki, *J. Agric. Food Chem.*, 2014, **62**, 1423−1448; (b) E. A. Baldwin, J. Bai, A. Plotto and S. Dea, *Sensors*, 2011, **11**, 4744-4766; (c) A. Riul Jr., C. A. R. Dantas, C. M. Miyazakic and O. N. Oliveira Jr., *Analyst*, 2010, **135**, 2481–2495.

2 (a) V. Rajasekharan, T. Stalin, S. Viswanathan and P. Manisankar, *Int. J. Electrochem. Sci.*, 2013, **8**, 11327-11336; (b) J. R. Araujo, C. B. Adamo, E. Robertis, A. Yu. Kuznetsov, B. S. Archanjo, B. Fragneaud, C. A. Achete and M.-A. De Paoli, *Compos. Sci. Technol.*, 2013, **88**, 106-112; (c) C. A. Mills, F. L. M. Sam, A. S. Alshammari, L. J. G. Emerson and S. R. P. Silva, *J. Display Technol.*, 2014, **10**, 125-131; (d) N. Rozanski, N. Chehata, A. Ltaief, R. Bkakri and A. Bouazizi, *Mater. Sci. Semicond. Process.*, 2014, **22**, 7-15; (e) W. Wang, G. Xu, X. T. Cui, G. Sheng and X. Luo, *Biosens. Bioelectron.*, 2014, **58**, 153-156; (f) D. S. Correa, E. S. Medeiros, J. E. Oliveira, L. G. Paterno and L. H. C. Mattoso, *J. Nanosci. Nanotechnol.*, 2014, **14**, 6509-6527; (g) C. Steffens, A. Manzoli, J. E. Oliveira, F. L. Leite, D. S. Correa and P. S. P. Herrmann, *Sens. Actuators, B*, 2014, **191**, 643–649.

3 (a) E. Song and J.-W. Choi, *Nanomaterials*, 2013, **3**, 498-523; (b) A. G. MacDiarmid, *Synthetic Met.*, 2001, **40**, 2581–2590.

4 S. Tian, J. Liu, T. Zhu and W. Knoll, *Chem. Mater.*, 2004, **16**, 4103-4108.

5 (a) S. Nasirian and H. M. Moghaddam, *Polymer*, 2014, **55**, 1866–1874; (b) J. Hu, M. Gan, L. Ma, Z. Li, J. Yan and J. Zhang, *Surf. Coat. Technol.*, 2014, **240**, 55-62.

6 (a) G. D. Khuspe, S. T. Navale, D. K. Bandgar, R. D. Sakhare, M. A. Chougule and V. B. Patil, *Electron. Mater. Lett.*, 2014, **10**, 191-197; (b) V. K. Shukla, P. Yadav, R. S. Yadav, P. Mishra and A. C. Pandey, *Nanoscale*, 2012, **4**, 3886-3893.

7 E. R. Carvalho, N. Consolin, A. Firmino, O. N. Oliveira Jr., L. H. C. Mattoso and L. Martin-Neto, *Sens. Lett.*, 2006, **4**, 129-134.

8 S. Srivastava and N. A. Kotov, *Acc. Chem. Res.*, 2008, **41**, 1831-1841.

9 X. Feng, Y. Liu, C. Lu, W. Hou and J-J. Zhu, *Nanotechnology*, 2006, **17**, 3578-3583.

10 L. Hao, C. Zhu, C. Chen, P. Kang, Y. Hu, W. Fan and Z. Chen, *Synthetic Met.*, 2003, **139**, 391–396.

11 P. Ghosh, A. Chakrabarti and S.K. Siddhanta, *Eur. Polym. J.*, 1999, **35**, 803-813.

12 N. Soltani, E. Saion, M. Erfani, K. Rezaee, G. Bahmanrokh, G. P. C. Drummen, A. Bahrami and M. Z. Hussein, *Int. J. Mol. Sci.*, 2012, **13**, 12412–12427.

13 (a) M. Raposo, R. S. Pontes, L. H. C. Mattoso and O. N. Oliveira Jr., *Macromolecules*, 1997, **30**, 6095-6101. (b) J. N. Hay, *Br. Polym. J.*, 1971, **3**, 74–82.

14 (a) M. L. Moraes, R. M. Maki, F. V. Paulovich, U. P. R. Filho, M. C. F. de Oliveira, A. Riul Jr., N. C. de Souza, M. Ferreira, H. L. Gomes and O. N. Oliveira Jr., *Anal. Chem.*, 2010, **82**, 3239–3246; (b) N. C. de Souza, J. R. Silva, R. Di Thommazo, M. Raposo, D. T. Balogh, J. A. Giacometti and O. N. Oliveira Jr., *J. Phys. Chem. B*, 2004, **108**, 13599-13606.

15 S. A. Travain, N. C. de Souza, D. T. Balogh and J. A. Giacometti, *J. Colloid. Interface Sci.*, 2007, **316**, 292-297.

16 Y. Haba, E. Segal, M. Narkis, G. I. Titelman and A. Siegmann, *Synthetic Met.*, 1999, **106**, 59–66.

17 M. J. Giz, S. L. A. Maranhão and R. M. Torresi, *Electrochem. Commun.*, 2000, **2**, 377–381.

18 (a) K. Huang and M. X. Wan, *Chem. Mater.*, 2002, **14**, 3486–3492; (b) P. A. McCarthy, J. Huang, S. C. Yang and H. L. Wang, *Langmuir*, 2002, **18**, 259–263.

19 C.-C. Chu, Y.-W. Wang, L. Wang and T.-I. Ho, *Synthetic Met.*, 2005, **153**, 321-324.

20 (a) S. Ivanov, V. Tsakova and A. Bund, *Electrochim. Acta*, 2013, **90**, 157–165; (b) X. Zhang, J. Zhu, N. Haldolaarachchige, J. Ryu, D. P. Young, S. Wei and Z. Guo, *Polymer*, 2012, **53**, 2109-2120; (c) J. Tarver, J. E. Yoo, T. J. Dennes, J. Schwartz and Y.-L. Loo, *Chem. Mater.*, 2009, **21**, 280–286; (d) C. Zhou, J. Han and R. Guo, *Macromolecules*, 2009, **42**, 1252-1257.

21 (a) W. Yan, X. Feng, X. Chen, W. Hou and J.-J. Zhu, *Biosens. Bioelectron.*, 2008, **23**, 925-931; (b) E. Granot, F. Patolsky and I. Willner, *J. Phys. Chem. B*, 2004, **108**, 5875-5881.

22 (a) J. E. Oliveira, V. P. Scagion, V. Grassi, D. S. Correa and L. H. C. Mattoso, *Sens. Actuators, B*, 2012, **171**, 249-255; (b) N. K. L. Wiziack, L. G. Paterno, F. J. Fonseca and L. H. C. Mattoso, *Sens. Actuators, B*, 2007, **122**, 484-492; (c) F. N. Crespilho, V. Zucolotto, J. R. Siqueira Jr., C. J. L. Constantino, F. C. Nart and O. N. Oliveira Jr., *Environ. Sci. Technol.*, 2005, **39**, 5385-5389.

23 S. Wold, K.P. Esbensen and P. Geladi, *Chemom. Intell. Lab. Syst.*, 1987, **2**, 37–52.

24 D. M. Taylor and A. G. Macdonald, *J. Phys. D: Appl. Phys.*, 1987, **20**, 1277-1283.

25 M. Ferreira, A. Riul Jr., K. Wohnrath, F. J. Fonseca, O. N. Oliveira Jr. and L. H. C. Mattoso, *Anal. Chem.*, 2003, **75**, 953-955.